REAL-TIME STRUCTURAL DAMAGE DETECTION USING WIRELESS SENSING AND MONITORING SYSTEM

Kung-Chun Lu[1], Chin-Hsiung Loh[2], Yuan-Sen Yang[3], Jerome P. Lynch[4] and K. H. Law[5]

Submit to

J of Smart Structural System

Date Submitted: May 12, 2007

Revised: January 30, 2008

[1] Graduate student, National Taiwan University, Taipei, Taiwan, r92521247@ntu.edu.tw

[2*] Professor, Department of Civil Engineering, National Taiwan University, Taipei, Taiwan, lohc0220@ccms.ntu.edu.tw **(corresponding author)**

[3]Associate Research Fellow, National Center for Research on Earthquake Engineering, Taiwan, ysyang@ncree.org.tw

[4]Assistant Professor, Department of Civil & Environmental Engineering, University of Michigan, Ann Arbor, MI 48109, USA, jerlynch@umich.edu

[5] Professor, Department of Civil & Environmental Engineering, Stanford University, Stanford, CA 94305, USA, law@stanford.edu

REAL-TIME STRUCTURAL DAMAGE DETECTION USING WIRELESS SENSING AND MONITORING SYSTEM

Kung-Chun Lu[1], Chin-Hsiung Loh[2], Yuan-Sen Yang[3], Jerome P. Lynch[4] and K. H. Law[5]

ABSTRACT

A wireless sensing system is designed for application to structural monitoring and damage detection applications. Embedded in the wireless monitoring module is a two-tier prediction model, the auto-regressive (AR) and the autoregressive model with exogenous inputs (ARX), used to obtain damage sensitive features of a structure. To validate the performance of the proposed wireless monitoring and damage detection system, two near full scale single-story RC-frames, with and without brick wall system, are instrumented with the wireless monitoring system for real time damage detection during shaking table tests. White noise and seismic ground motion records are applied to the base of the structure using a shaking table. Pattern classification methods are then adopted to classify the structure as damaged or undamaged using time series coefficients as entities of a damage-sensitive feature vector. The demonstration of the damage detection methodology is shown to be capable of identifying damage using a wireless structural monitoring system. The accuracy and sensitivity of the MEMS-based wireless sensors employed are also verified through comparison to data recorded using a traditional wired monitoring system.

Keywords: Structural health monitoring, wireless sensing and monitoring module, damage detection, AR-ARX model,

INTRODUCTION

Structural monitoring systems that detect damage in large structures, such as buildings and bridges, can improve safety and reduce maintenance costs. The design of such systems is the goal of structural health monitoring (SHM). Many existing SHM techniques attempt to detect damage by continuously monitoring structural responses originating from ambient excitation. To avoid the problems inherent to wired monitoring systems (*e.g.*, difficult installations, high costs), researchers have recently demonstrated that wireless sensing networks can be successfully used for structural health monitoring [1,2]. The advantages of using wireless monitoring systems is that they are: 1) easy to install, 2) accurate with wireless data identical to data collected from a tethered data acquisition system, and 3) highly reliable with little to no data loss in the wireless channel. These merits show that MEMS sensors and wireless sensing units have great potential for use in future automatic SHM and damage detection systems.

From the theoretical viewpoint, damage detection using data generated by structural monitoring systems has been extensively studied over the past 30 years and the literature on the subject is rather immense. Doebling *et al*. [3] gives a comprehensive survey of vibration based global damage detection techniques. Various approaches on data analysis for system identification and damage detection have been proposed in the literature. In the parametric identification method, Kondo and Hamamoto [4] used an ARMA (Auto-Regressive Moving Average) model to identify the modal frequencies and modal shapes of the structure and detect the location of damage from changes of the curvature of mode shapes. Safak [5,6] used ARMAX (Auto-Regressive Moving Average with eXogenous) models with RPEM (Recursive Prediction Error Model) to identify the real structure of linear time-varying systems. Andersson [7] used AFMM (Adaptive Forgetting through Multiple Models) methods to trace time-varying parameters of the structure. Loh and Lin [8] also used off-line and on-line identification techniques to accurately determine time-varying system parameters. Recently, an advanced damage detection approach using time series analysis of vibration signals was proposed by Los Alamos National Laboratory (LANL) [9]. The method proposed is based on the "statistical pattern recognition" paradigm; the method is attractive for adoption within an automated monitoring system. Following their initial work, a procedure based on the time series analysis of vibration signals for damage detection and localization within a mechanical system was proposed by Sohn *et al*. [10]. In this method the standard deviation of

the residual error, which is the difference between actual measured structural responses and those predicted from a two-stage combination of the AR and ARX models, is used as the damage-sensitive feature to locate damage.

At the present stage, advanced embedded system technologies offer the structural engineering community low-cost yet reliable wireless sensors with powerful computational cores for local damage detection [11~13]. In this study, a wireless monitoring system assembled from wireless sensor prototypes proposed by Wang *et al.* [2] was installed on a full-scale RC frame structure with and without brick walls and used to measure system responses during shaking table testing in the laboratory. A damage detection method proposed by Sohn and Farrar [10] was adopted and embedded in the wireless sensing unit to continuously identify the structural damage situation in real time during the shaking table test. With a flexible and capable hardware design, the wireless sensing unit can easily execute the computational tasks required by a SHM and damage detection system. Based on the calculation of the AR-ARX model coefficients by the wireless sensing and monitoring system, the damage feature of the structural system is assessed. A graphical user interface visualization system, in connection with the wireless sensor network, is also implemented in this damage detection system for on-line and real time monitoring.

COMMUNICATION PROCEDURE FOR TWO-TIER TIME SERIES DAMAGE DETECTION

Approaches based upon the statistical pattern recognition paradigm proposed by Sohn *et al.* 2001[10] and extended by Lynch *et al*. 2002 [14], appear promising and easy to implement in the computational core of a wireless sensing unit to detect structural damage that occurs at different stages. The wireless sensing and monitoring modular system (WiMMS) is shown in ***Fig. 1***. The design of the wireless sensing unit is optimized for the application of structural monitoring and includes three major subsystems: the sensing interface, the computational core, and the wireless communication system. The sensing interface is responsible for converting analog sensor signals on multiple channels into 16-bit digital formats. The digital data is then transferred to the computational core by a high-speed serial peripheral interface (SPI) port. Abundant external memory (128 kB) is associated with the computational core for local data storage and analysis. The hardware profile and functional design of the WiMMS system is

shown in ***Fig. 1*** [14]. The Maxstream XStream wireless modem, operating on the 2.4 GHz wireless band is used for peer-to-peer communication between sensors and between sensors and the data repository.

The damage detection monitoring system contains one wireless sensing unit with MEMS accelerometers interfaced to collect the response of the structure and one receiver unit (server) outside of the structure to coordinate the system. By integrating the damage detection algorithm upon the wireless sensing unit, the wireless monitoring system can be used for on-line damage detection of the structure. The on-line damage detection algorithm and data broadcast between the sensing unit and the receiver (server) is described as follows:

1. The wireless sensing unit continuously collects a series of ambient vibration of structural responses and broadcasts the collected structural responses to the receiver (to the server side). This ambient signal will serve as the reference data of the structure.

2. Under the assumption of a stationary response time history of the structure at a single measurement location (for the case of a white noise excitation), an autoregressive (AR) time series model is fit to the response data, *y(t)*,

$$y_m(k) = \sum_{i=1}^{p} \phi_i y_m(k-i) + r^m{}_{AR}(k) \qquad (1)$$

where ϕ_i is the *i*-th AR coefficient, *p* is the order of the AR model (*p*=22 is assumed in this study), $r_{AR}(k)$ is the residual error and *m* indicates *m*-th time series. For a given model order, it is generally assumed that the residual error between the measurement and the prediction from the AR model is mainly caused by the unknown external input. Since "m" sets of response data has been collected, a set of reference AR coefficients can be obtained for the structure. It is important to identify the suitable model order for the AR model. Improper selection of model order may influence the residual error term, $r_{AR}(k)$. A plot of response prediction error with respect to the model order must first be developed. As shown in **Figure 2**, the vector norm of the residual error time history of the AR model is plotted as the "loss function" versus the model error. Based on these identified AR models, one can select a suitable one as a reference model (with a high probability of occurrence). The collected data corresponding to the selected AR model (or the reference model) will be used as the reference database.

3. The residual error, $r^n{}_{AR}(k)$, from Eq. (1) will be used as the background (or environmental signal) noise. Therefore, with this selected reference data set, an ARX model is employed to reconstruct the input/output relationship between $r^n{}_{AR}(t)$ and $y_n(t)$:

$$y_n(k) = \sum_{i=1}^{a} \alpha_i y_n(k-i) + \sum_{j=0}^{b} \beta_j r^n{}_{AR}(k-j) + \varepsilon^n{}_{ARX}(k) \quad (2)$$

where α and β are the coefficients of the ARX model, and *a* and *b* are the order of the ARX model (in this study *a*=12 and *b*=10 are assumed). The final residual error of the ARX model, $\varepsilon^n{}_{ARX}$, is defined as the damage sensitive feature of the structure [10]. This model parameter estimation procedure is conducted at the server with the AR-ARX model parameters archived as a valid reference model of the structure in its undamaged state. An extensive library of AR-ARX models, all of the same model size, corresponding to the undamaged structure is generated by exciting the structure with different levels of ambient excitation.

4. For the structure in an unknown structural state, a new set of ambient vibration data of the structure is measured from the wireless sensing unit after an earthquake excitation. An AR model of the same order (*p*=22) is fit to the new recorded ambient signal, $\tilde{y}(k)$.

$$\tilde{y}(k) = \sum_{i=1}^{p} \tilde{\phi}_i y(k-i) + \tilde{r}_{AR}(k) \quad (3)$$

This estimation is conducted in the wireless sensing unit and broadcast to the server.

5. At the sever, the newly received AR coefficients are compared with each AR model of the signal from the reference database (as shown in Eq. (1)) so as to select a reference model most closely associated with the unknown structure's AR model. To select the suitable reference model, it is defined by minimizing the following difference of the AR coefficients:

$$difference = \sum_{i=1}^{p} (\phi_i - \tilde{\phi}_i)^2 \quad (4)$$

The minimum value of the difference in Eq. (4) will be used as a means of selecting the bets AR-ARX model pair. Once selected, the ARX model coefficients and the standard deviation of $\varepsilon^n{}_{ARX}(k)$ of the reference AR-ARX model pair are broadcast to sensing unit.

5. The wireless sensing unit on the structure will receive the selected ARX model coefficients from sever and determine the residual error of the reference ARX model using the unknown structure's time history response.

$$y_{np}(k) = \sum_{i=1}^{a} \alpha_i y_{np}(k-i) + \sum_{j=0}^{b} \beta_j r^n{}_{AR}(k-j) + \tilde{\varepsilon}^{np}{}_{ARX}(k) \quad (5)$$

The standard deviation of the ARX model residual error, $\sigma(\tilde{\varepsilon}_{ARX})$, using the newly measured data (or signal from the damaged signal) is determined. The residual error ratio is then calculated:

$$h = \sigma(\tilde{\varepsilon}_{ARX}) \Big/ \sigma(\varepsilon_{ARX}) \quad (6)$$

6. The sensing unit broadcasts the ratio *h* to the server. The server then decides if the structure is damaged based on the ratio. For example, if the unknown structural state is undamaged, then the anticipated ratio will be near 1. However, if damage has occurred in the structure, then none of the reference AR-ARX models will fit the damage structural response well. The result will be a damage ratio is exceeding 1.

Fig. 3 shows the major program flow of the damage detection strategy in a wireless monitoring system. The AR-ARX time series damage detection method is well suited for automated execution by a wireless monitoring system since no data is shared between wireless sensors and calculations are self-contained to each wireless sensor.

TEST STRUCTURES

To verify the proposed on-line damage detection technique using wireless sensing units, shaking table tests on three different types of reinforced concrete (RC) frame structures exposed to different levels of base excitation are conducted. Three sets of near full-scale RC frames were designed, constructed and tested at the National Center for Research on Earthquake Engineering (NCREE) in Taipei, Taiwan, to study the dynamic behavior of RC frames without and with infill brick walls (along the out-of-plane direction of the ground motion). The three different RC frames are specified as: (1) Frame A1F, (2) Frame P1F, and (3) Frame B1F. Frame A1F is an RC frame with two 12cm thick post-laid brick walls. As shown in ***Fig. 4a*** (top view), the A1F structure consists of four RC columns, a strong top floor, a strong foundation and two side walls. The distances between the center lines of the columns along the X and Y directions are 2.1m and 3.05m, respectively. The height of the columns is 2.8m. The column section is 0.35 by 0.3m with eight #5 longitudinal steel bars and #3 transverse ties with spacing of 0.25m. The nominal strength of the concrete and steel are 180kg/cm^2 and 2800kg/cm^2, respectively. The 10-ton top floor and the 13-ton foundation are both designed to be strong compared with the columns and are considered as rigid diaphragms herein. Accelerometers (Setra 141A with a maximum range of ±4g) are installed at the top and base of the structure while four linear variable differential transformer (LVDT) displacement measurement devices are positioned on each brick wall so as to measure the deformation of the wall, as shown in ***Fig. 4b***. Preliminary modal analysis using displacement-based beam-column elements with fiber sections using OpenSees (ver. 1.7.1) [15] reveal the dominant natural period of the specimen is 0.24sec. Frame P1F is designed with the same details as frame A1F but without infill walls. Another 2-story RC frame structure is also

designed for this study. The detailed design drawings of this structure are shown in ***Fig. 5***. The dominant frequency of this 2-story RC frame is 12.0 Hz. ***Fig. 6*** shows the photos of the three frame structures tested.

There are three objectives in this study: 1) to assess the accuracy of the wireless monitoring system, 2) to utilize the computational capabilities of the wireless sensing unit for continuous real time damage detection, 3) to evaluate the reliability of the damage detection algorithm and the capabilities of the visualization system for real time structural health monitoring. Both conventional wired sensors and the wireless sensing unit are installed on each specimen to monitor their response induced by the shake table. To quantify the accuracy of the wireless monitoring system, the laboratory data acquisition system (Pacific Instrument Series 5500 data acquisition classis) is also used to offer high-resolution data acquisition with a sample rate of 200 Hz. In the wireless monitoring system, a sampling rate of 100Hz is used. To excite these three structures, respectively, various intensities of base excitations are applied by the shaking table. It should be noted that the white noise and seismic ground motion records are applied back to back sequentially in a uni-axial direction. **Table 1** summarizes the excitations during the laboratory study for each of the structural specimens. The response of the test structures to the ground motion of the Chi-Chi 1999 earthquake collected at the TCU078 seismic station are used for this study. Comparisons between the recorded roof acceleration response of the wired and wireless system reveal nearly identical results. Comparison of the floor acceleration collected from both the wired and wireless systems were also verified. From the recorded acceleration response of the frame structure during earthquake excitation, the restoring force diagrams of different test stages are also examined. ***Fig. 7*** shows the restoring force diagram of the three structures for different levels of excitation. From the restoring force diagram corresponding to the different test cases, inelastic hysteretic behavior can be observed for case of large excitations.

DAMAGE DETECTION THROUGH THE EMBEDDED AR-ARX SYSTEM

Real-time damage detection using the two-tier damage detection model

The first set of tests is intended to calibrate the residual error ratio of Eq. 6 to different levels of seismic damage in the RC frame structures. Towards this end, a reference database of AR-ARX model pairs corresponding to the undamaged structure must first be populated. For the undamaged structure, the acceleration response of the roof during white noise

excitation (normalized to 50 gals peak ground acceleration) is collected. After each test, the wireless sensor communicates with the server and is commanded to determine the AR-ARX model pair for the undamaged structure. Once the reference database is established, an AR-ARX model pair is fit using ambient white noise response data for the structure after damage has been introduced by a seismic ground motion. Following the procedures in the previous section, the ratio of AR-ARX two-tier model residual errors can be generated for each damage states. ***Table 1*** archives the estimation of the residual error ratio based on the white noise test data of the three structures (i.e., wall frame (A1F), pure frame (P1F) and the 2-story RC frame (B1F) structures). From all three structural systems, the ratio of residual error increases in tandem with the increasing earthquake excitation level. In essence, the residual error ratio is a good indicator of the degree of damage in the structure. From the observation of Table 1, it is found that the residual error calculated after earthquake excitation with peak acceleration of 1000 gals is much larger than one which indicates severe damage was developed in the frame structure after the earthquake excitation with peak acceleration of 1000 gal.

Results from off-line AR-ARX model residual analysis

In order to verify the accuracy of the damage detection methodology embedded in the computational cores of the wireless monitoring system's sensor, the data collected from the wired data acquisition system (i.e. the NCREE data acquisition system) is also used to conduct the damage detection analysis off-line using the same two-tier damage detection algorithm. ***Fig. 8*** plots the ratio of AR-ARX two-tier model residual error for the three test structures for different test cases using the ambient vibration data (each test data was separated into 6 different segments). It is observed that the estimated residual error is consistent with the results from the on-line real-time damage detection system tabulated in Table 1. However, the off-line data analysis yields AR-ARX two-tier model residual error ratios slightly larger than those obtained from wireless sensing unit. This slight difference can be attributed to the difference in the sampling rate between these two systems (100Hz for wireless sensing unit and 200Hz for wireless system). Therefore, the estimated residual error is different depending upon whether data is collected by the wireless or tethered systems. Regardless, the results all indicate the residual error ratio exceeds one when the structure is damaged (for excitation larger than 1000 gal) and increases in tandem with damage.

DAMAGE DETECTION VERIFICATION USING SEISMIC RESPONSE MEASUREMENTS

To verify the accuracy of the real-time damage detection strategy using a two-tier time series model, the seismic response data from the different intensity levels of base excitation are processed using an alternative strategy. Specifically, a wavelet analysis and an extended Kalman filter estimation method are both applied to estimate the stiffness degradation of the three frame systems during the application of seismic excitation.

Wavelet Packet Transform (WPT) The wavelet packet transform (WPT) is one extension of the discrete wavelet transform (DWT) that provides complete level-by-level decomposition [16~19]. It is assumed that $c_j^i(t)$ is the giving i-th wavelet packet component at the *j-th* level of decomposition. The amplitude $a_j(t)$ and the instantaneous phase function $\theta_j(t)$ are defined as:

$$a_j^i(t) = \sqrt{\{c_j^{i\,2}(t) + c_j^{i\,(H)^2}(t)\}} \tag{7}$$

where $c_j^{i(H)}(t)$ is the Hilbert transform of $c_j^i(t)$. Based on Eq. (7), the Hilbert amplitude spectrum can be constructed using the acceleration response data. ***Fig. 9a*** and ***Fig.9b*** show the frequency-time Hilbert amplitude spectrum of the A1F and P1F frame structures using their acceleration responses. Through the comparison of the response data from the ground excitations with peak accelerations of 150 and 1000 gal, the change in the dominant system frequency is self-evident. The Hilbert marginal spectrum, HMS, (with respect to the. *j-th* level) is also investigated which is defined as:

$$H_j(f_i) = \int a^i{}_j(t)\, dt \qquad where \qquad f_i = (2i-1)\, f_N / 2^{j+1} \tag{8}$$

as applied to the calculated Hilbert marginal spectrum. ***Fig. 10*** shows the HMS of the earthquake response data of the two structural systems (A1F and P1F). f_i is the central frequency of the *i-th* component function of j-level WPT. It is clear that f_i moves to the lower frequency for the data correspond to the larger excitation. The change of dominant frequency in the Hilbert marginal spectrum with respect to the ratio of residual error estimated from ambient vibration data is clearly identified, as shown in ***Fig. 11***. It is clear that the estimated ratio of residual error has a direct relationship with the change of structural natural frequency. It is also observed that the residual value changes very quickly for the structural system subjected to the 1000 gal intensity (or higher) of ground excitation.

Kalman Filter Technique for Identification To estimate the change of structural model parameters, such as stiffness, during earthquake excitation, the Kalman estimation method can be used [20-21]. Based upon the developed adaptive covariance matrix of the estimation error, an error index is introduced in which the abrupt change of modal parameters can be identified. Through the calculation of error index, defined as the ratio between the current modified error covariance matrix and the temporal average of error covariance, and incorporated with the pre-assigned threshold the adaptive factor can be employed in the Kalman filter estimation algorithm to detect and quantify the change of system parameter [22]. ***Fig. 12*** shows the identified stiffness (assumed as that corresponding to a SDOF system) of the two structural systems from the seismic response data under different earthquake excitation intensity. ***Fig. 13*** plots the estimated ratio of residual error with respect to the identified floor stiffness from the different stages of base excitation. This relationship provides a physical meaning for the residual error in relating the structural stiffness reduction to changes in the residual error ratio. ***Fig. 14*** shows the photo taken from the experiments of different test stage of wall frame structure. Significant cracks at the both end of the column and major cracking distributed across columns with brick wall partially collapse can be observed for larger intensity of excitation (such as 1000 gals and 1500 gals).

INTEGRATION OF WIMMS AND LABVIEW (VISUALIZATION)

LabVIEW is a popular graphical programming language widely used in the design of data acquisition systems. There are three basic communication subroutines written in LabVIEW as "Visualized Interpretation (VI)" function blocks: receive wireless package, transmit wireless unsigned short, and transmit wireless single float (as shown in ***Fig. 15***) VI's. In this study three major programs are developed under LabVIEW using the aforementioned VI's: real-time display, presentation of the results of the AR model estimation and presentation of the results of damage detection strategy (as shown in ***Fig. 16***). In ***Fig. 16***, there are three pages to display. Page1 (as shown in ***Fig. 16a***) displays the real time response time history and moving window Fourier amplitude spectrum. Page 2 (as shown in ***Fig. 16b***) displays the results of the embedded AR analysis which includes the AR coefficients (as broadcast by the wireless sensing unit), the roots of the transfer function, the poles of the transfer function plotted upon the polar coordinate and the natural frequencies which are extract by considering the complex valued poles of the transfer function upon the complex plane polar coordinate system. Page 3 (as shown in ***Fig. 16c***) displays the coefficients of the AR-ARX model, and the ratio of the

residue error which is received wirelessly from the wireless sensing unit. With this setup, the real-time presentation of structural response and the residual error calculated by the real-time damage detection using the two-tier damage detection model can be viewed by engineers and facility owners.

CONCLUSIONS

This research work has explored the use of wireless sensing units for structural health monitoring applications. The wireless sensing system has been specially designed for applications in structural monitoring and damage detection. Embedded in the wireless monitoring module, a two-tier time series prediction model based upon auto-regressive (AR) and autoregressive model with exogenous inputs (ARX) time series models is used for obtaining the damage sensitive feature of the structure in real time. This approach is basically using the ambient vibration measurement of the structure after the excitation of earthquake to estimate the post-seismic condition of the structure (*i.e.* existence and degree of damage). In order to validate the approach, both seismic response data of a series of shaking table tests of three different RC frame structures and data from low-level white noise excitations are used to estimate the damage. Through this study the following conclusions can be drawn:

1. The two-tier damage detection model provides a very convenient and easy to apply method within the computational core of a wireless sensing unit for damage detection using ambient vibration response signal. The damage index can be estimated immediately after the ambient vibration survey of the structure and communicated to the appropriate decision makers.
2. Comparison on the damage estimation method using the AR-ARX model from ambient vibration response data and using wavelet analysis from seismic response data directly shows good consistent. The two-tier time series damage detection method together with the wireless sensing unit can provide real-time damage assessment.

ACKNOWLEDGMENTS

This research was supported by National Science Council, Taiwan, under grant number NSC 95-2625-Z-002-032 and NSC 94-2915-I-492-C08. Technical and experimental supports from National Center for Research on Earthquake Engineering are much appreciated.

REFERENCES

1. Ying Lei, Anne S. Kiremidjian, K. Krishnan Nair, Jerome P. Lynch and Kincho H. Law, "Algorithms for time synchronization of wireless structural monitoring sensors," *Earthquake Engng. Struct. Dyn*. 34, 555-573, 2005.

2. Wang, Y., Lynch, J. P. and Law, K. H., "A wireless structural health monitoring system with multithreaded sensing devices: design and validation," *Structural and Infrastructure Engineering*, in press, 2005.

3. Doebling, S. W., Farr, C. R., Prime, M. B., and Shevitz, D. W., "Damage identification and health monitoring of structural and mechanical systems from changes in their vibration characteristics: A literature review," Los Alamos National Laboratory, Tech. Rep., May, 1996.

4. Kondo, I. and T. Hamamoto, "Seismic damage detection of multi-story building using vibration monitoring", *Eleventh World Conference on Earthquake Engineering*, 1996, Paper No. 988

5. Safak, E., "Adaptive modeling, identification, and control of dynamic structural systems: I - Theory", *Journal of Engineering Mechanics, ASCE*, Vol.115(11), 1989 ,pp.2386-2405.

6. Safak, E., "Adaptive modeling, identification, and control of dynamic structural systems: II - Application", *Journal of Engineering Mechanics, ASCE*, Vol.115(11), 1989 ,pp.2406-2426.

7. Andersson, P., "Adaptive forgetting in recursive identification through multiple models", *Int. J. Control*, Vol.42, No.5, 1985, pp.1175-1193

8. Loh, C. H. and H. M. Lin, "Application of off line and on line identification techniques to building seismic response data" *Earthquake Engineering and Structural Dynamics*, Vol.25, No.3, 1996,pp.269-290.

9. Sohn, H., Farrar, C. R., Hunter, N. And Worden, K. "Applying the LANL statistical pattern recognition paradigm for structural health monitoring to data from a surface-effect fast patrol boat," Los Alamos National Laboratory Report No. LA-13761-MS, University of California, Los Alamos, NM, 2001.

10. Sohn, H. and Farrar, C. R., "Damage diagnosis using time series analysis of vibration signals," *Smart Materials and Structures*, 10, 446-451, 2001.

11. Lynch, J. P., Sundararajan, A., Law, K. H., Kiremidjian, A. S. and Carryer, E., "Embedding damage detection algorithms in a wireless sensing unit for attainment of operational power efficiency," *Smart Materials and Structures*, 13(4), pp. 800-810, 2004.

12. Lei, Y., Kiremidjian, A. S., Nair, K. K., Lynch, J. P., Law, K. H., Kenny, T. W., Carryer, E., and Kottapalli, A., "Statistical damage detection using time series analysis on a structural health monitoring benchmark problem," *Proc. 9th International conference on Application of Statistics and Probability in Civil engineering ICAPS-9*, San Francisco, US, 2003.

13. Lynch, J. P., Wang, Y, Lu, K. C., Hou, T. C. and Loh, C. H., "Post-seismic damage assessment of steel structures instrumented with self-interrogating wireless sensors," *Proc. of the 8-th U.S. National Conf. on Earthquake Engineering*, paper No. 1390, San Francisco, US, April, 2006.

14. Lynch, J. P., Sundararajian, A., Law, K. H. and Kiremidjian, A. S., Kenny, Thomas and Carryer, Ed, "Computational Core Design of a Wireless Structural Health Monitoring system," Proceedings of Advances in Structural Engineering and Mechanics (ASEM'02), Pusan, Korea, August 21~23, 2002.

15. McKenna, F. and Fenves, G. L., "An Object-oriented Software Design for Parallel Structural Analysis," *Proceedings of Advanced Technology in Structural Engineering, Structures Congress 2000,* Philadelphia, Pennsylvania, USA, May 8-10. (Software available at http://opensees. berkeley.edu/), 2000.

16. Corbin, M., Hera, A. and Hou, Z., "Locating damages using wavelet approach," Proc. 14th Engineering Mechanics Conf. (EM2000), (CD Rom), Austin, TX, 2000.

17. Hou, Z., Noori, M. and St.Amand, R., "Wavelet-based approach for structural damage detection", ASCE, J. Eng. Mech. Div., Am. Soc. Civ. Eng., 12(7), p.677-683, 2000.

18. Yen, Gary G. and Lin, Kuo-Chung, "Wavelet packet feature extraction for vibration monitoring", IEEE, 47(3), p.650-667, 2000.

19. Sun, Z. and Chang, C. C., "Structural damage assessment based on wavelet packet transform", ASCE, J. Struct. Eng., 128(10), p1354-1361, 2002.

20. Jann N. Yang, Silian Lin, Hongwei HUang and Li Zhou, "An Adaptive Extended Kalman Filter for Structural Damage Identification," Structural Control & Health Monitoring, 2006; 13; 849-867.

21. Jann N. Yang, Silian Lin, and Li Zhou "Identification of Parametric Changes for Civil Engineering Structures Using An Adaptive Kalman Filter", Smart Structures and Materials, 2004, Vol. 5391, 389-399

22. Shieh-Kung Huang, Chin-Hsiung Loh, Wen I. Liao, and Jann N. Yang, "On-line Tracking Techniques of Structural Parameters Based on Adaptive Kalman Filter Algorithm," submitted, 2008.

Table 1a: Estimation of the ratio of residual error through wireless damage detection module (for case of wall frame structure: A1F)

Wall Frame (A1F)		Ratio of residual error
Excitation	Intensity	
White Noise 1	50 gal	Reference
TCU078EW	150 gal	
White Noise 2	50 gal	0.902
TCU078EW	500 gal	
White Noise 3	50 gal	1.027
TCU078EW	1000 gal	
White Noise 4	50 gal	1.377
TCU078EW	1500 gal	
White Noise 5	50 gal	1.545

Table 1b: Estimation of the ratio of residual error through wireless damage detection module (for case of pure frame structure: P1F).

Pure Frame (P1F)		Ratio of residual error
Excitation		
White Noise 1	50 gal	Reference
TCU078EW	150 gal	
White Noise 2	50 gal	0.955
TCU078EW	500 gal	
White Noise 3	50 gal	0.930
TCU078EW	1000 gal	
White Noise 4	50 gal	2.354
White Noise 5	50 gal	1.706
White Noise 6	50 gal	1.407
TCU078EW	1500 gal	
White Noise 7	50 gal	1.616
TCU078EW	1800 gal	
White Noise 8	50 gal	3.003

Table 1c: Estimation of the ratio of residual error through wireless damage detection module (for case of pure frame structure:B1F).

Excitation		Ratio of residue error
White Noise 1	50 gal	Reference
TCU078EW	200 gal	
White Noise 2	50 gal	1.018
TCU078EW	400 gal	
White Noise 4	50 gal	1.102
TCU078EW	600 gal	
White Noise 5	50 gal	1.064
TCU078EW	800 gal	
White Noise 6	50 gal	1.206
TCU078EW	1000 gal	
White Noise 7, 8,	50 gal	1.659
TCU078EW	1200 gal	
White Noise 9	50 gal	1.638
TCU078EW	1500 gal	
White Noise 10, 11	50 gal	2.176
TCU078EW	2000 gal	
White Noise 12	50 gal	2.410
TCU078EW	1200 gal	
White Noise 13	50 gal	2.609

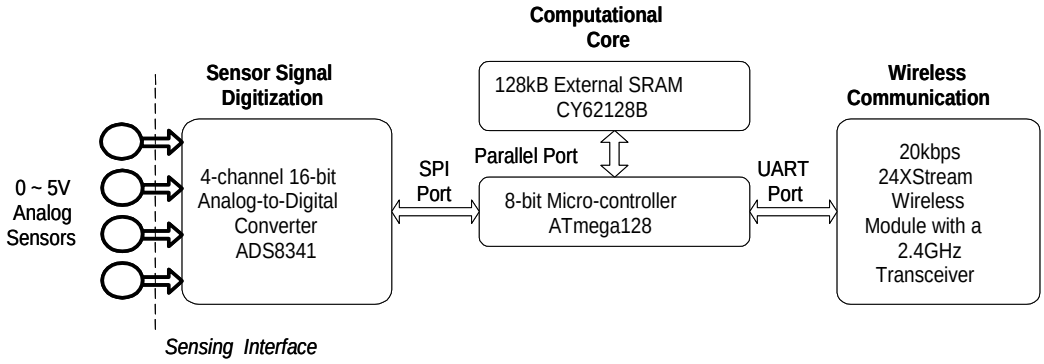

Figure 1: Hardware architecture design of wireless sensing and monitoring system [11].

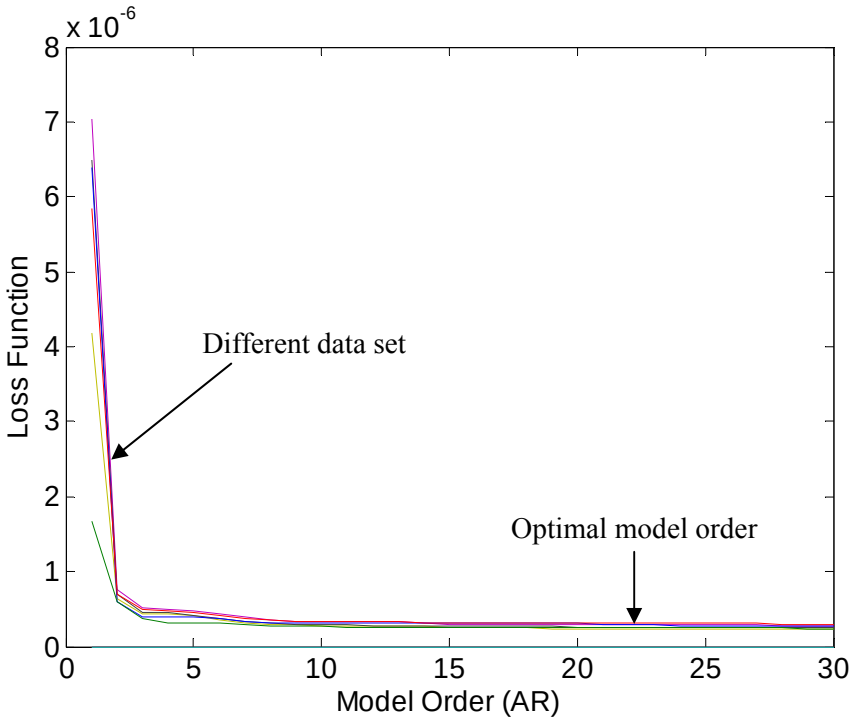

Figure 2; Plot of loss function with respect to the order of AR model.

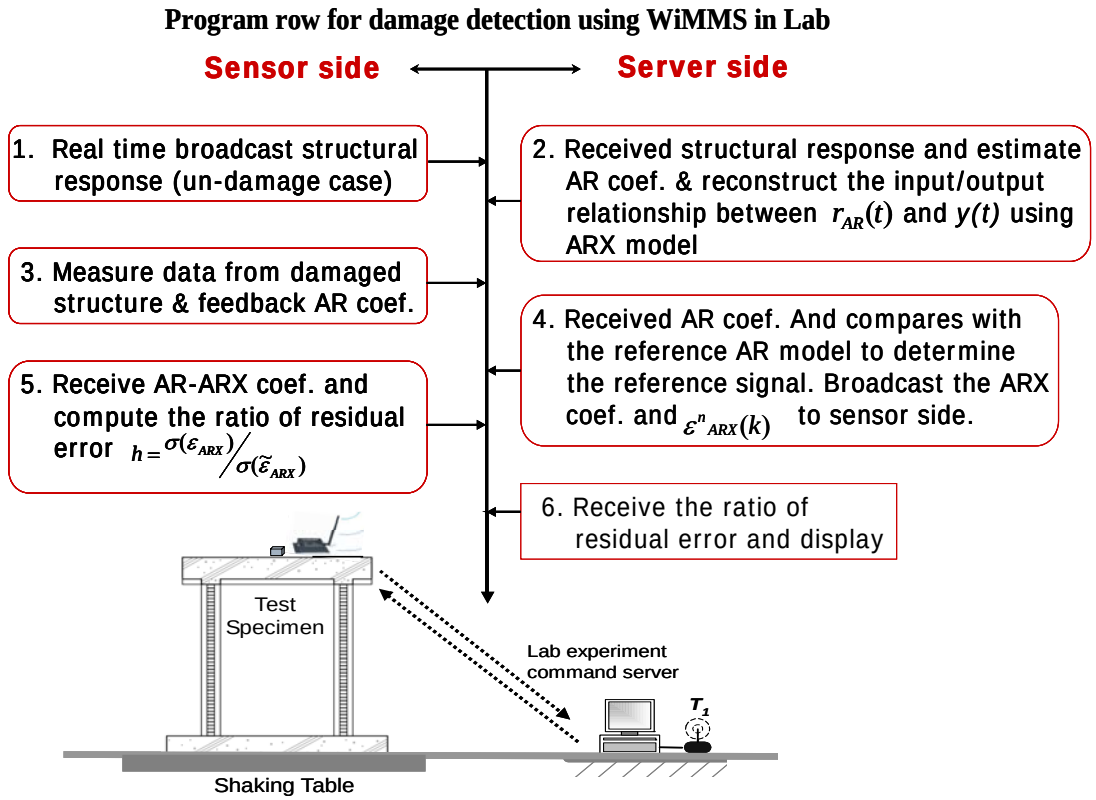

Figure 3: Implementation of the AR-ARX damage detection strategy in a wireless monitoring system to conduct the continuous damage detection of large structural testing in the laboratory.

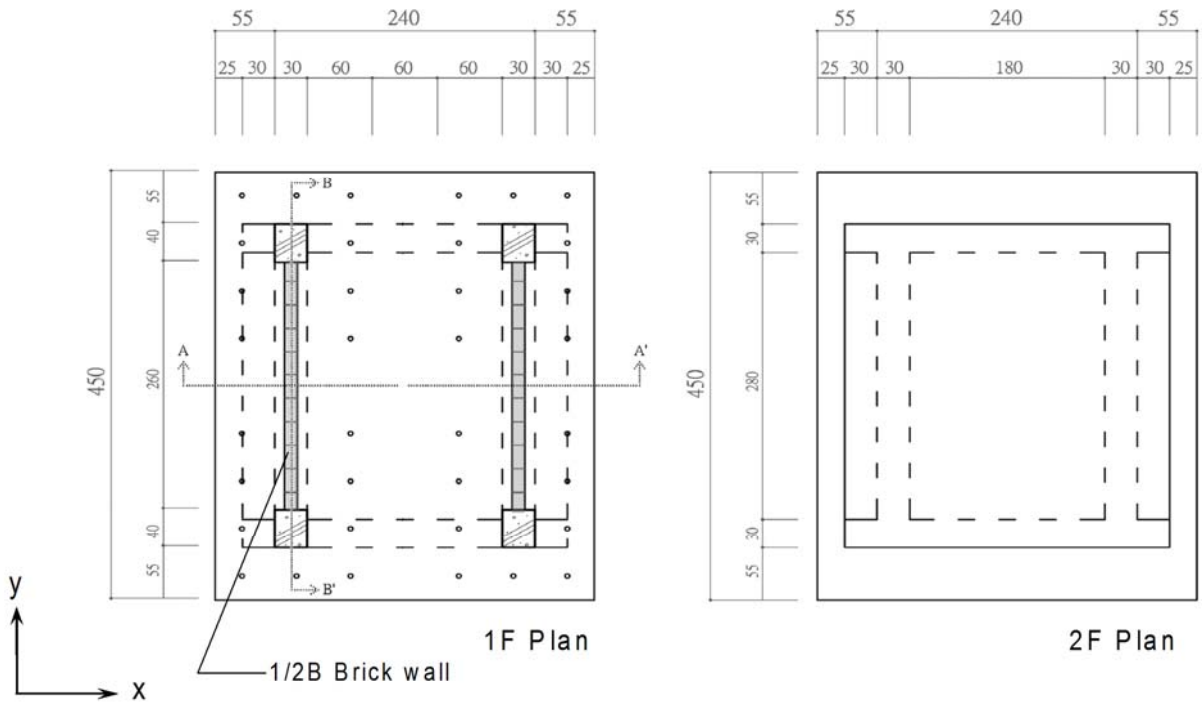

Figure 4: (a) Top view of the test specimen (A1F).

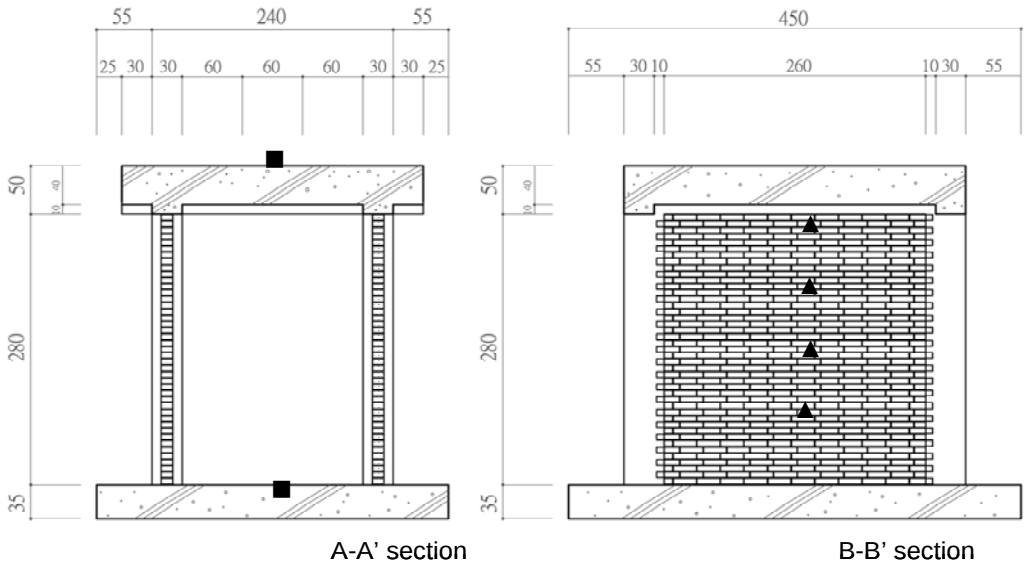

Figure 4: (b) Side view of the test specimen. Locations of accelerometers (■) and LVDT (▲) are also shown.

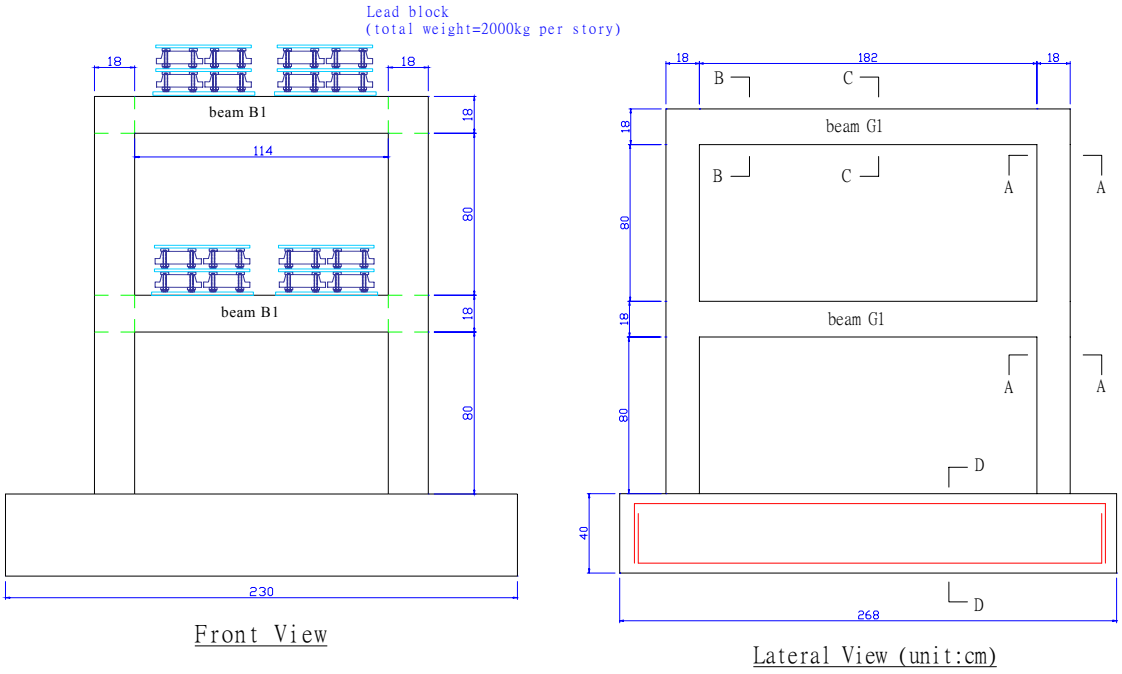

Figure 5: Draft of the front view and side view of the two-story RC frame.

(a)

(b)

(c)

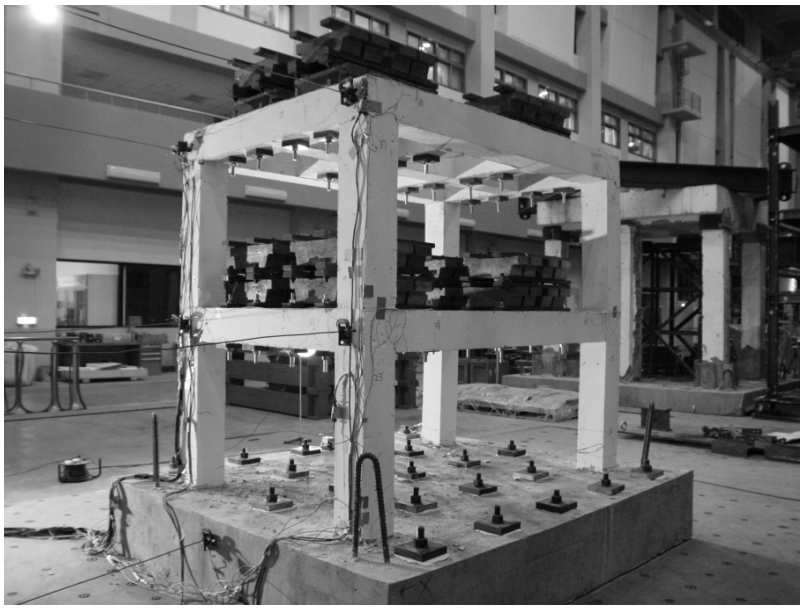

Figure 6: (a) Photo of the specimen A1F frame, (b) Photo of the specimen P1F frame, (c) Photo of the 2-story RC frame structure.

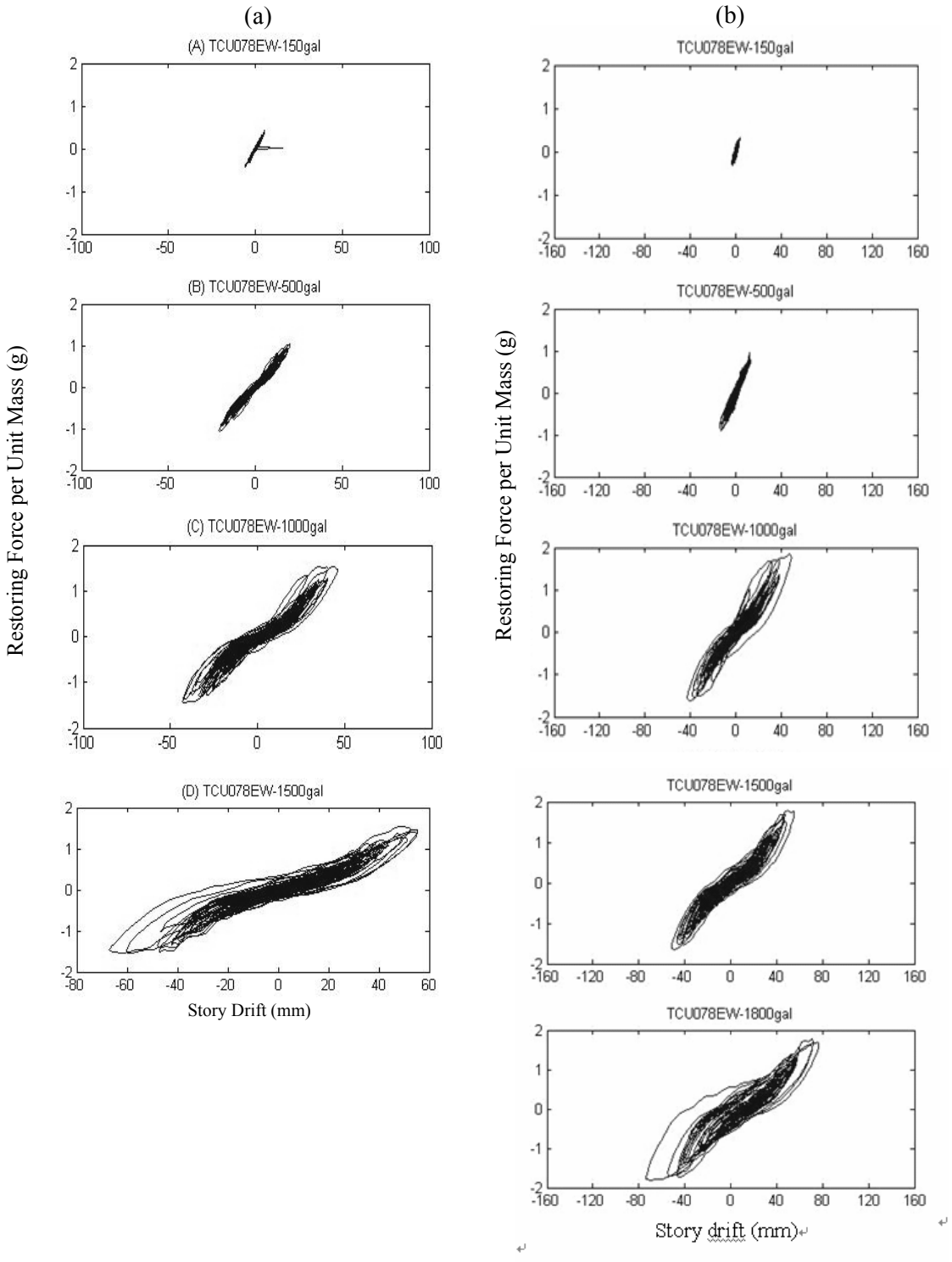

Figure 7a and b: Restoring diagram of the test structure from different input excitation level (150gal, 500gal, 1000gal and 1500 gal), (a) A1F structure, (b) P1F structure.

(C)

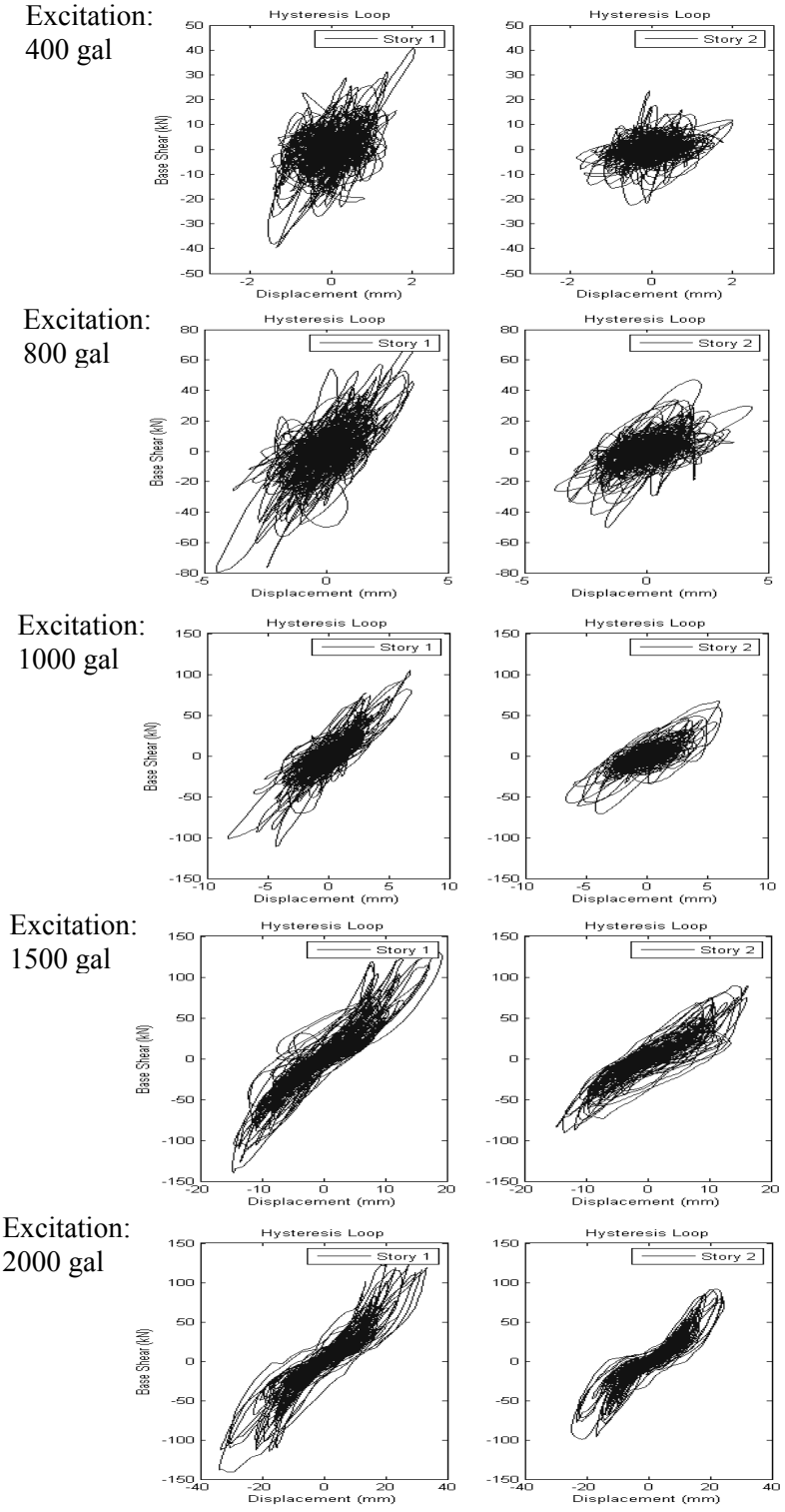

Figure 7c: Restoring diagram of the test structure from different input excitation level (400gal, 800gal, 1000gal, 1500 gal and 2000gal) for (c) B1F structure.

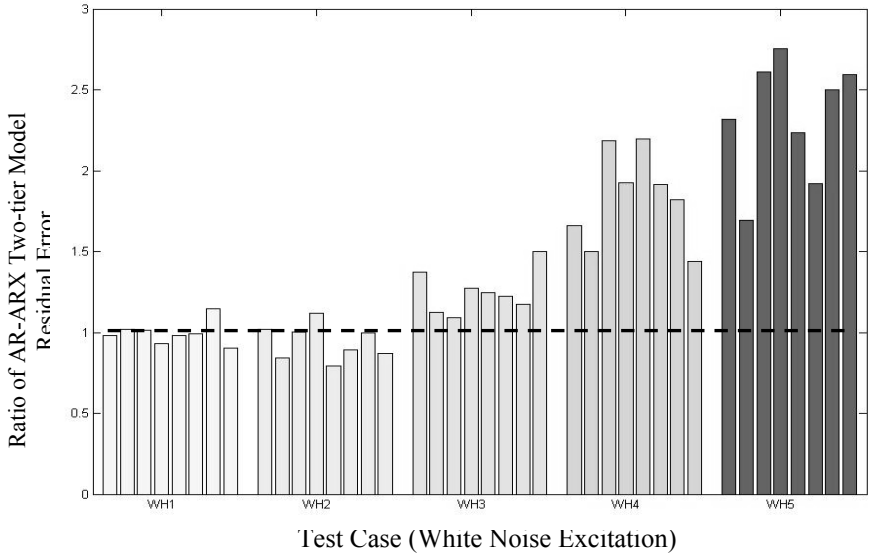

Figure 8a: Ratio of AR-ARX two-tier model residual error from test of RC frame (A1F) in filled with 1/2B post-laid brick walls (using off-line data).

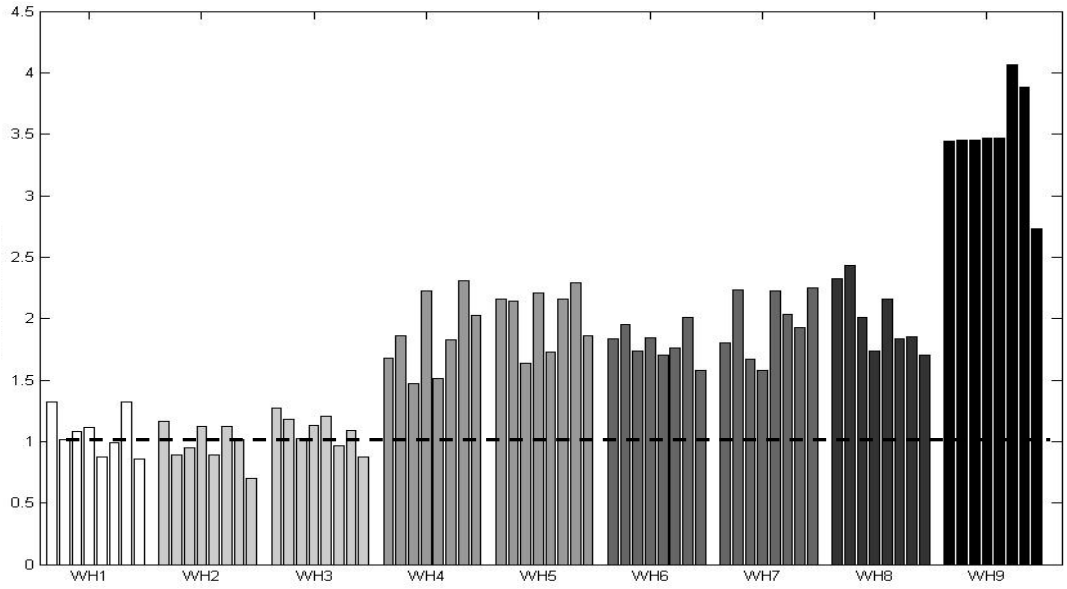

Figure 8b: Ratio of AR-ARX two-tier model residual error from test of RC frame without walls (P1F).

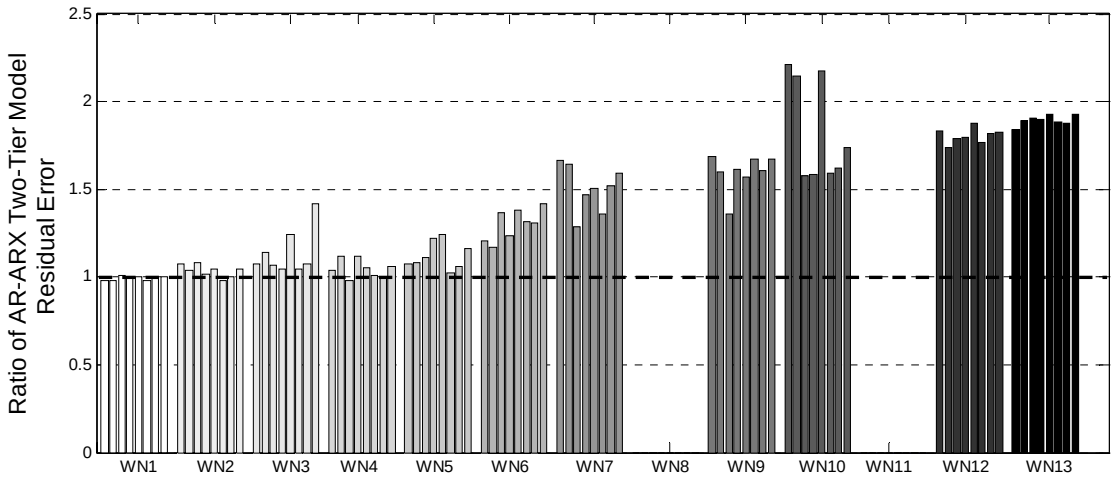

Figure 8c: Ratio of AR-ARX two-tier model residual error from test of 2-story RC frame without walls (B1F).

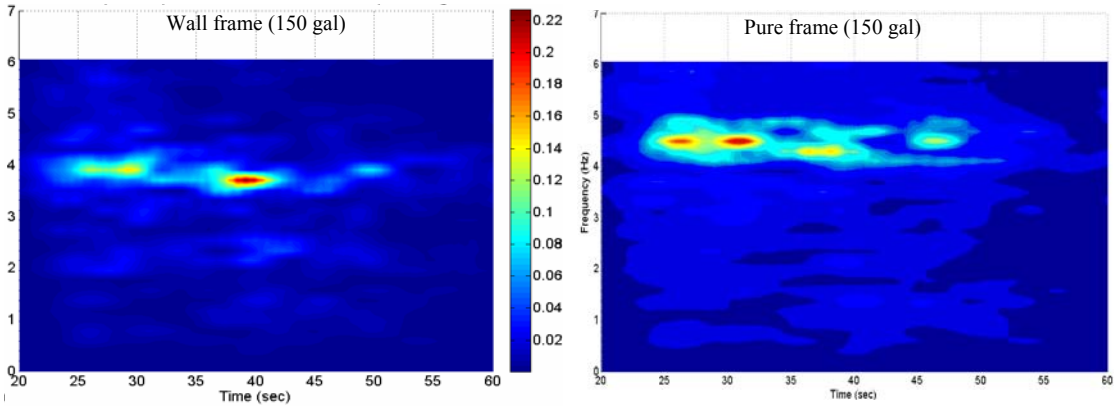

Figure 9a: Frequency-time-Hilbert amplitude spectrum of roof acceleration response of A1F and P1F frame structures (for case of 150 gal excitation).

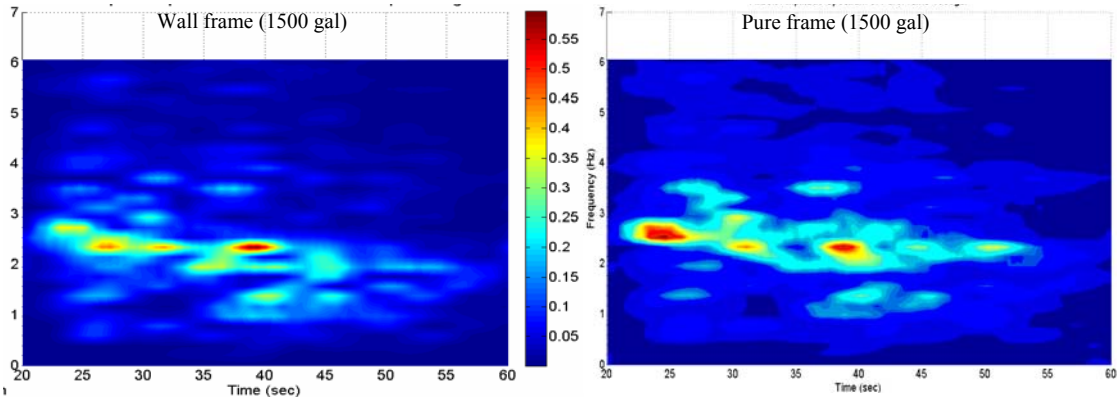

Figure 9b: Frequency-time-Hilbert amplitude spectrum of roof acceleration response of A1F and P1F frame structure (for case of 1500 gal excitation).

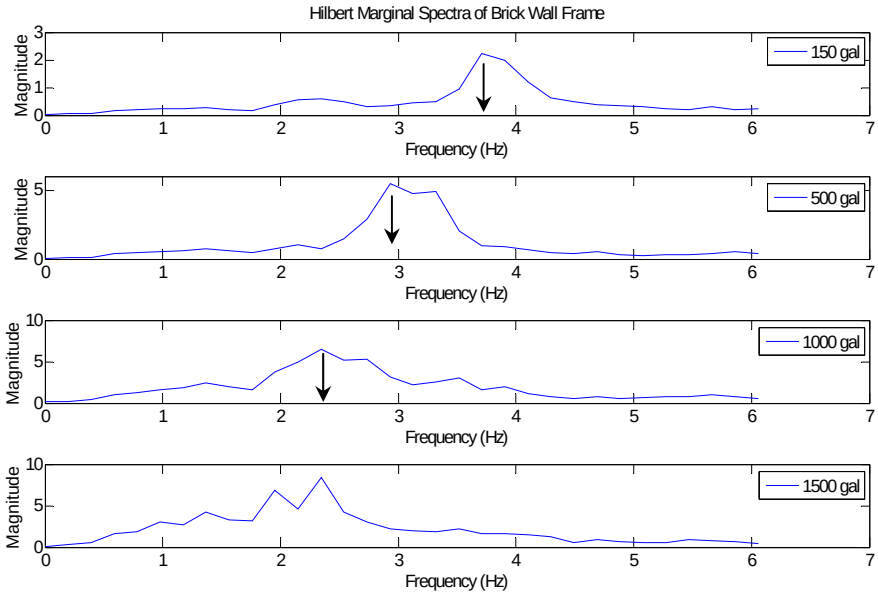

Figure 10a: Hilbert amplitude spectrum of four earthquake response data of A1F structure (150gal, 500gal, 1000gal and 1500gal).

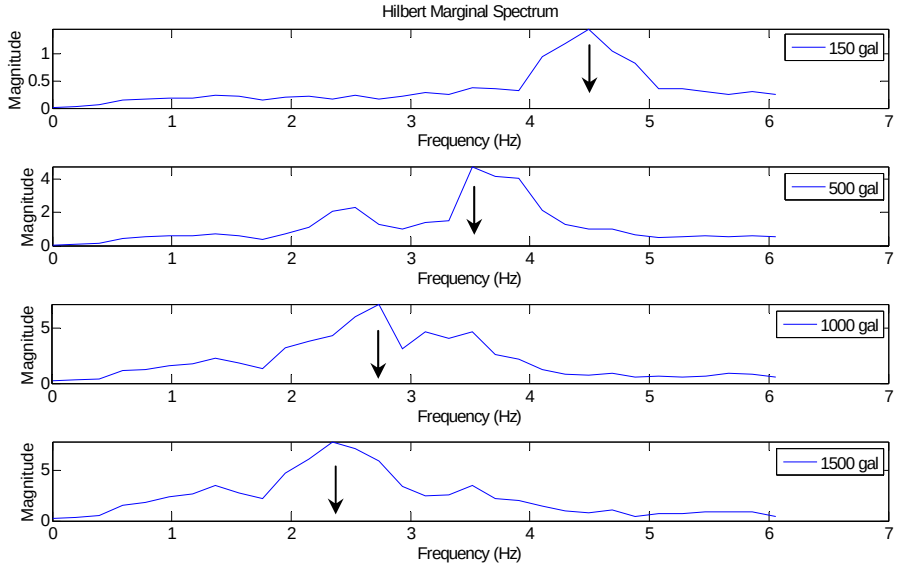

Figure 10b: Hilbert amplitude spectrum of four earthquake response data of P1F structure (150gal, 500gal, 1000gal and 1500gal).

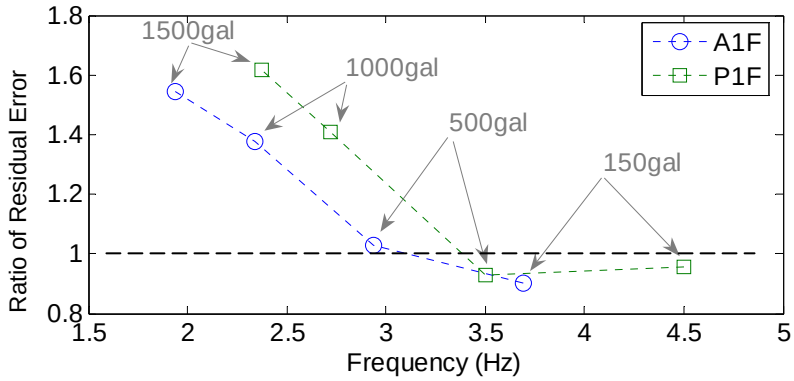

Figure 11: Plot of the estimated ratio of residual error from four different sets of ambient data with respect to system dominant frequency (the acceleration number shown in the figure indicated the intensity level of input excitation .

(a) A1F structure

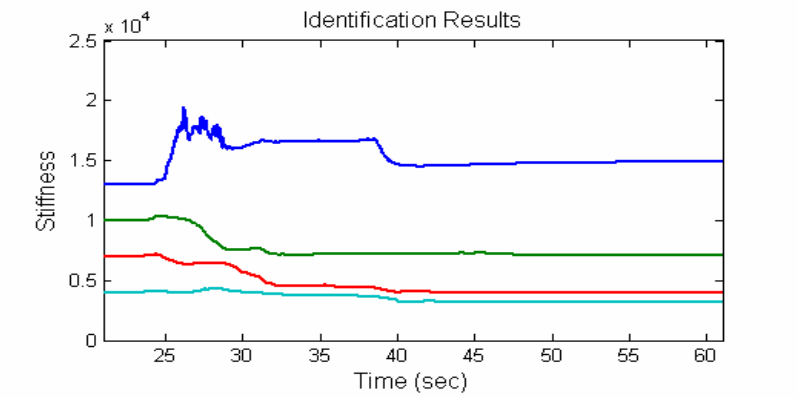

(b) P1F structure

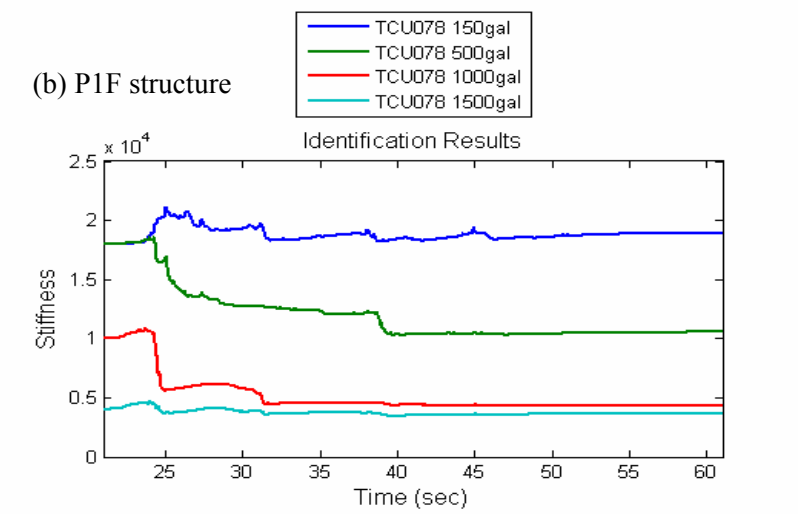

Figure 12: Estimated time-varying system stiffness from four different sets of earthquake response data, (a) A1F structure, (b) P1F structure.

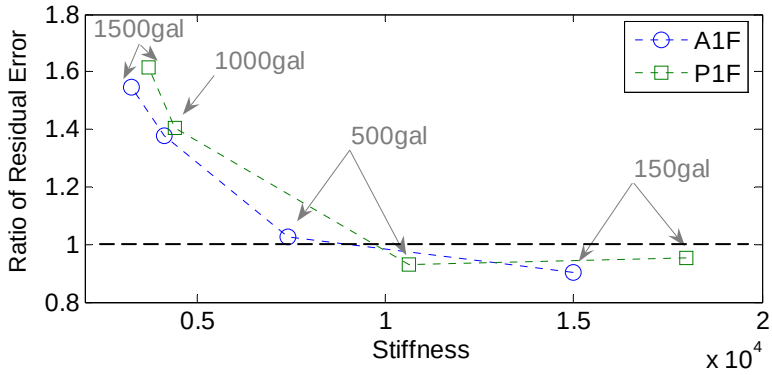

Figure 13: Plot of ratio of residual error from four different sets of ambient data with respect to the identified system stiffness.

150 gal	500 gal	1000 gal	1500 gal
			
			

Figure 14: Photos taken at the column location of A1F wall frame structure after different intensity level of excitations.

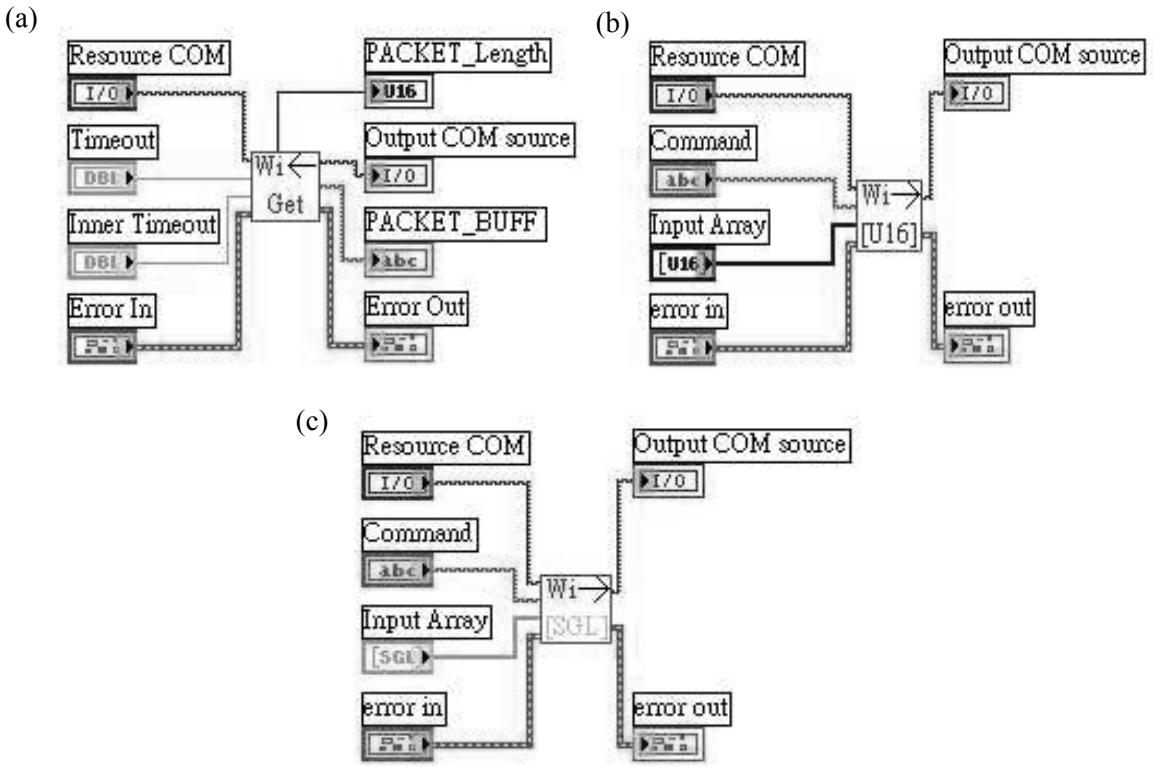

Figure 15: (a) Receive Wireless Package VI, (b) Transmit Wireless Unsigned short, (c) Transmit Wireless single float.

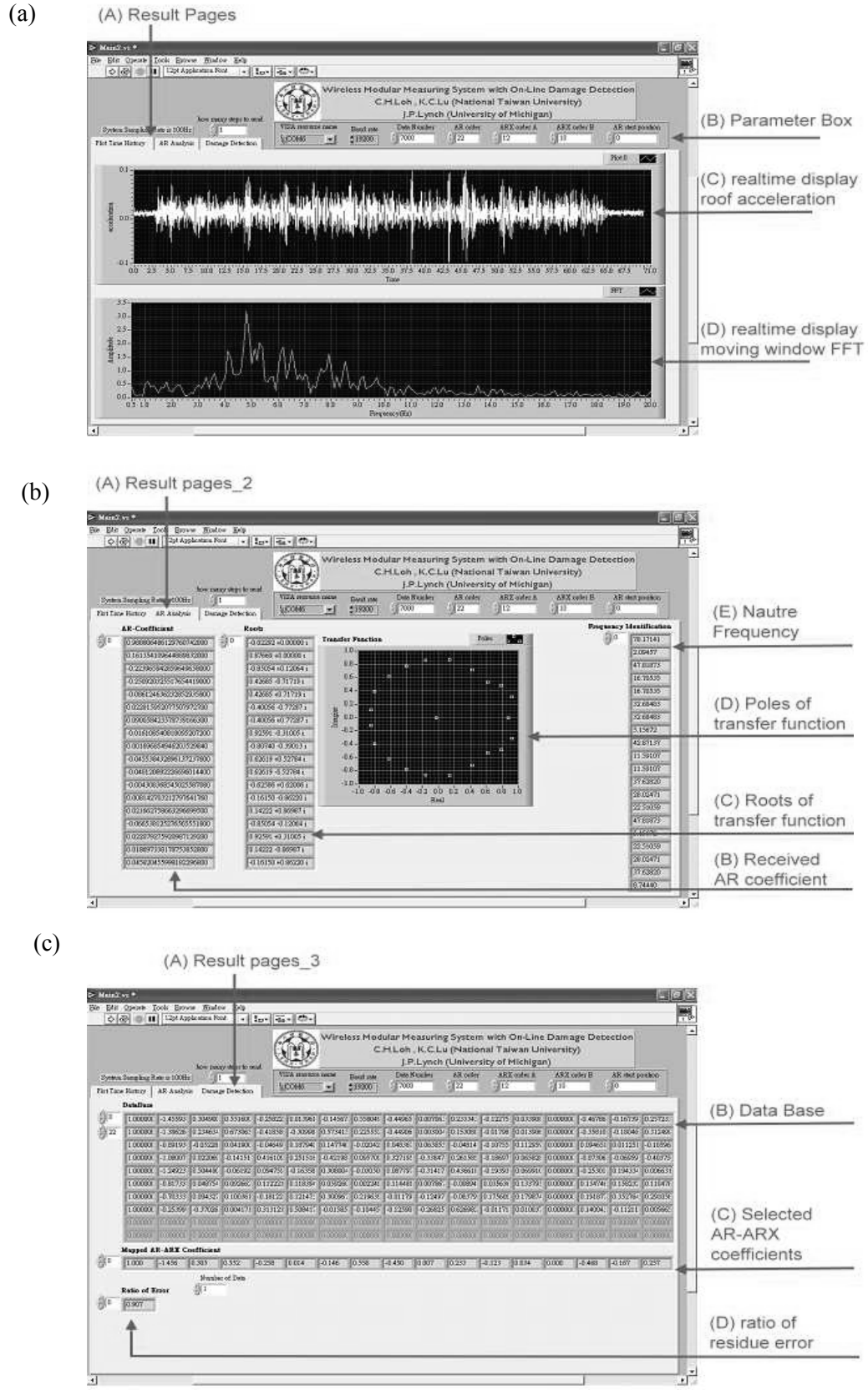

Figure 16: Three pages to display from the wireless health monitoring system: (a) Real-time display, (b) AR analysis, (c) Damage Detection.